Experimental observations of fracture dissolution: The role of Peclet number on evolving aperture variability

Russell L. Detwiler,[1] Robert J. Glass,[2] and William L. Bourcier[1]

Received 24 March 2003; revised 8 May 2003; accepted 20 May 2003; published 27 June 2003.

[1] Dissolution of the surfaces of rock fractures can cause significant alteration of the fracture void space (aperture) and fracture permeability (k). Both surface reaction rates and transport of reactants within the fracture can limit local dissolution. We investigated the role of Peclet number (Pe), a measure of the relative importance of advective and diffusive transport of reactants, on fracture dissolution in two identical transparent analog fractures with different initial values of Pe (Pe_o). High-resolution light-transmission techniques provided direct measurements of the evolving aperture field during each experiment. For Pe_o = 54 distinct dissolution channels formed, while for Pe_o = 216 we measured minimal channeling and a reduction in short wavelength aperture variability. The nature of the dissolution patterns strongly influenced the relative increase in k. A 110% increase in the mean aperture due to dissolution resulted in estimated permeability increases of 440% and 640% for the Pe_o = 54 and Pe_o = 216 experiments, respectively. *INDEX TERMS:* 5104 Physical Properties of Rocks: Fracture and flow; 5114 Physical Properties of Rocks: Permeability and porosity; 1829 Hydrology: Groundwater hydrology; 1832 Hydrology: Groundwater transport. **Citation:** Detwiler, R. L., R. J. Glass, and W. L. Bourcier, Experimental observations of fracture dissolution: The role of Peclet number on evolving aperture variability, *Geophys. Res. Lett.*, *30*(12), 1648, doi:10.1029/2003GL017396, 2003.

1. Introduction

[2] Fractures provide dominant pathways for flow and transport in the subsurface though they typically account for only a small portion of the total porosity. Flow of a reactive fluid can cause dissolution of the rock surfaces resulting in significant alteration of fracture apertures (b) and changes in permeability (k). Fracture dissolution is limited by reaction rates at the fracture surfaces and reactant transport within the fracture. The Damkohler (Da) and Peclet (Pe) numbers parameterize the relative magnitude of these processes. Da weighs the relative influence of surface reaction rates to advective transport of reactants ($Da = K_s/V$, where K_s is the reaction rate constant and V is the mean fluid velocity) and Pe weighs the relative magnitude of advective and diffusive transport of reactants ($Pe = V\langle b\rangle/D_m$, where $\langle b\rangle$ is the mean aperture and D_m is the molecular diffusion coefficient of the reactants).

[3] In fractures with local reaction kinetics that are fast relative to reactant transport (large Da) fracture dissolution will be transport limited and strongly influenced by Pe. Three-dimensional reactive transport simulations in numerical models of fractures clearly demonstrated that Pe could have a strong influence on dissolution patterns [*Bekri et al.*, 1997]. At low Pe, diffusion controlled dissolution resulted in the growth of large disconnected cavities and a slow increase in k, whereas for high Pe, advection dominated reactant transport resulted in aperture growth along dominant flow channels and a more rapid increase in k. However, due to the complexity of the three-dimensional computational model used for these simulations, the scale was limited (~several spatial correlation lengths). Using a simplified two-dimensional reactive transport model, *Hanna and Rajaram* [1998] demonstrated that in a larger fracture (~15 correlation lengths) aperture variability could lead to reaction front instabilities and the growth of distinct dissolution channels that strongly affect the rate of increase of k. A recently developed lattice-Boltzmann-based fracture dissolution model [*Verberg and Ladd*, 2002] allows fully three-dimensional simulations in fractures that are large relative to the correlation scale of the aperture field, and has the potential to yield further insights into the conditions that lead to dissolution-channel formation and the influence on k.

[4] Efforts to evaluate the results of computational investigations have been limited due to the difficulty of experimentally measuring dissolution-induced changes in aperture variability. Surface profilometry measurements of dissolution-induced changes to the surfaces of a 4.7 × 7.2-cm fractured calcite core demonstrated the formation of a single fracture-scale channel and small-scale smoothing of the fracture surfaces [*Durham et al.*, 2001]. By contrast, experiments designed to investigate the influence of density gradients on dissolution when the influent solution was far from chemical equilibrium demonstrated increased small-scale roughness with no channeling [*Dijk et al.*, 2002]. These latter experiments used nuclear magnetic resonance imaging to measure aperture changes in three, 1.8 × 3.6-cm fractured halite cores. Differences in scale, reaction kinetics, transport processes, initial fracture geometries, and confining stresses, as well as heterogeneous surface chemistry, each may have contributed to these disparate results.

[5] To elucidate the role of individual parameters on fracture dissolution, we have designed an experimental system in which we can vary parameters independently. We present results from a pair of experiments in fractures that are much larger than the spatial correlation scale of the aperture fields. The fracture geometry and reaction kinetics are identical in the fractures so the results provide a direct interrogation of the influence of transport processes (Pe) on

[1]University of California, Lawrence Livermore National Laboratory, USA.
[2]Flow Visualization and Processes Laboratory, Sandia National Laboratories, USA.

0094-8276/03/2003GL017396$05.00

the dissolution-induced evolution of fracture apertures and permeability.

2. Experimental Design

[6] We fabricated two analog fractures by mating the same 9.9 × 15.2 cm textured glass surface with equal-sized, flat, transparent potassium-dihydrogen-phosphate (KDP) crystals. Flow through these fractures alters only the KDP surface, so mating the same rough glass surface with another flat surface produces a fracture with an identical initial aperture field. Rigid no-flow boundaries along the long edges of the fractures and inflow and outflow manifolds along the short edges of the fracture fixed the relative position of the two surfaces. Thus, dissolution of the KDP surface did not cause closure of the fracture (i.e. zero confining stress).

[7] Because the fractures were transparent, light transmission techniques [*Detwiler et al.*, 1999], provided high spatial resolution (1192 × 1837, 0.083 × 0.083 mm pixels) measurements of dissolution-induced changes in b over the entire flow field during experiments. We measured the initial aperture field by mating the rough glass surface with a non-reactive, flat, transparent surface using the procedures described by *Detwiler et al.* [1999]. Using a non-reactive surface to measure the initial aperture field prevented possible alteration of the fracture during the measurement process, resulting in accurate (±2 μm) measurements of the initial aperture field. Figure 1 shows the initial aperture field. The mean $\langle b \rangle$ and standard deviation (σ_b) of the measured aperture field are 0.126 and 0.049 mm, respectively, and the field is isotropic and stationary with a spatial correlation length (λ) of ~0.8 mm (~10 pixels).

[8] Constant-head reservoirs connected to the inflow and outflow manifolds controlled the hydraulic gradient during the experiments and a balance recorded the cumulative mass of outflow. Between the inflow reservoir and the inflow manifold, the tubing passed through a constant temperature bath to maintain the influent temperature at 27.5°C. The equilibrium concentration (C_s) of KDP in water at 27.5°C is 25.6% by weight and D_m is approximately 6.77×10^{-6} cm^2/s (based upon the data of *Mullin and Amatavivadhana* [1967]). We used an influent concentration, C_{in}, of 24.1% by weight (0.95 C_s) to replicate near equilibrium conditions prevalent in many geologic systems and to avoid large density gradients, which can influence reactant transport [*Stockman*, 1997] and fracture dissolution [*Dijk et al.*, 2002]. The density difference between C_{in} and C_s was ~0.9% (based upon the data of *Mullin and Amatavivadhana* [1967]), and local density gradients are likely much smaller. The influent solution was also dyed with 1/16 g/l of FD&C Blue #1 (Warner Jenkinson) to increase the light absorbance of the solution.

[9] A charge-coupled-device (CCD) camera recorded the intensity of light transmitted through the transparent fracture over the duration of each experiment. To measure dissolution-induced changes to the fracture aperture we used the Beer-Lambert law,

$$I = I_o \exp(-\varepsilon c_{dye} b) \quad (1)$$

where I is the transmitted light intensity measured at a pixel of the CCD corresponding to an 0.083 × 0.083 mm portion of the fracture, I_o is the reference intensity at the same location (fracture saturated with dye free solution), b is the local aperture, and c_{dye} and ε are the concentration and absorbance coefficient of the light absorbing solute, respectively. The CCD camera measured changes in light intensities caused by aperture growth. By measuring the light transmitted through the fracture at the beginning of the experiment, $I_{t=0}$, and intensities at later times, I_t, the change in local aperture, Δb_t, at each pixel of the field can be quantified by modifying the Beer-Lambert law to yield

$$\Delta b_t = \ln(I_{t=o}/I_t)\varepsilon c_{dye} \quad (2)$$

This approach requires a value for εc_{dye}, which we quantified during measurement of the initial aperture field. Implicit in this approach is that the absorbance of the solute is linear over the range of measured apertures. Analysis of dye-absorbance nonlinearity in similar fractures [*Detwiler et al.*, 1999] demonstrates that for a 1/16 g/l dye concentration, apertures of 1 mm (largest aperture during these experiments) are underestimated by less than 1%. Also, we estimate that this modified procedure for measuring changes in aperture results in additional measurement uncertainty of ±1.5% of Δb_t. Comparison of the measured $I_{t=0}$ fields for the two experimental fractures confirmed that the two fractures were indistinguishable.

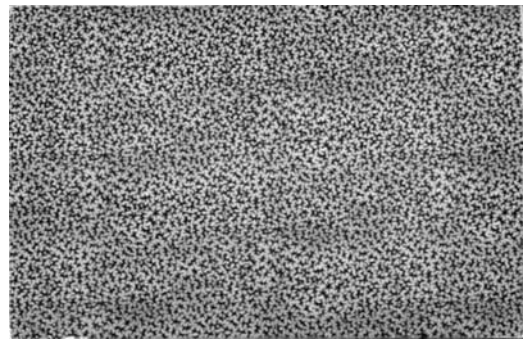

Figure 1. Initial 9.9 × 15.2 cm aperture field measured at 0.083 × 0.083 cm resolution using light transmission techniques. The grayscale represents the magnitude of the aperture with black = 0 and white ≥ 0.025 cm.

3. Results

[10] For the two experiments, the constant head reservoirs were adjusted to establish hydraulic gradients of ~4% and 16%, which yielded initial flow rates of 0.0145 and 0.0036 cm^3/s. These flow rates correspond to initial values of Pe (Pe_o) of 216 and 54. In both experiments, increases in the fracture aperture caused by dissolution resulted in a steady increase in flow rate. However, the two experiments resulted in dramatically different dissolution patterns. Figure 2 shows dissolution-induced aperture growth in each fracture after $\langle b \rangle$ had increased from 0.126 mm to 0.260 mm. At Pe_o = 54, the aperture grew significantly along the inflow edge of the fracture until instabilities along the evolving dissolution front led to the formation of discrete dissolution channels. These channels initiated as thin tendrils following connected regions of large aperture

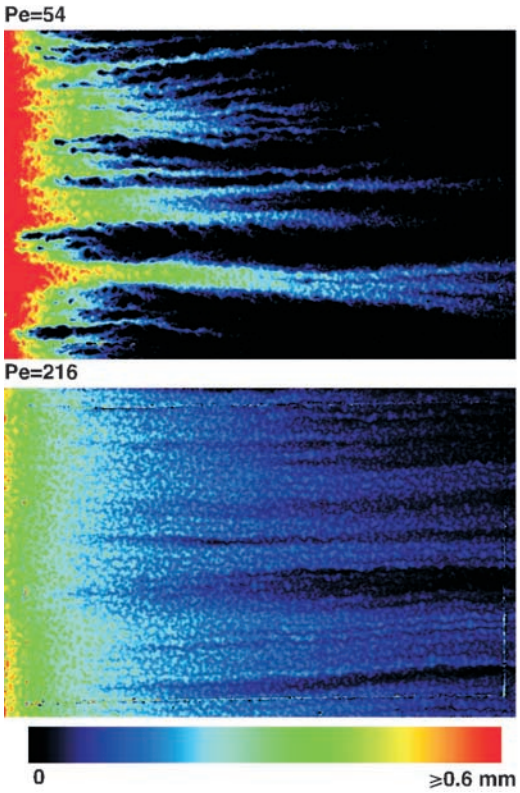

Figure 2. Dissolution-induced aperture growth when $\langle b \rangle$ = 0.26 mm for the Pe_o = 54 and 216 experiments, respectively. The color scale represents the increase in aperture. Flow was from left to right.

then grew laterally as local apertures increased causing locally enhanced flow rates. At Pe_o = 216, dissolution occurred more uniformly over the width of the fracture, with small-aperture regions dissolving more rapidly, resulting in reduced short-wavelength variability of the aperture field. For the Pe_o = 54 and Pe_o = 216 experiments, σ_b increased from 0.0049 mm to 0.0200 mm and 0.0104 mm, respectively.

[11] Comparing histograms and semivariograms of the initial aperture field to those of the aperture fields at $\langle b \rangle$ = 0.260 mm provides a more detailed look at the dissolution-induced changes to the fracture aperture field. The histograms plotted in Figure 3 demonstrate that the Pe_o = 54 experiment resulted in a significant increase in the magnitude of the largest apertures and a small increase in the

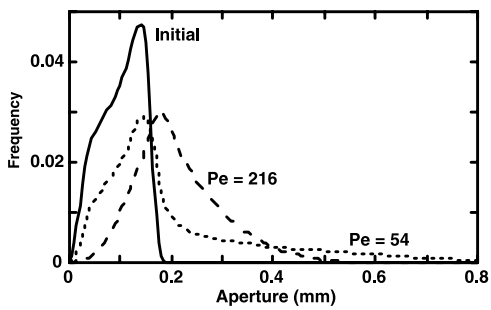

Figure 3. Histograms of aperture distribution before dissolution experiments (Initial) and when $\langle b_o \rangle$ = 0.26 mm.

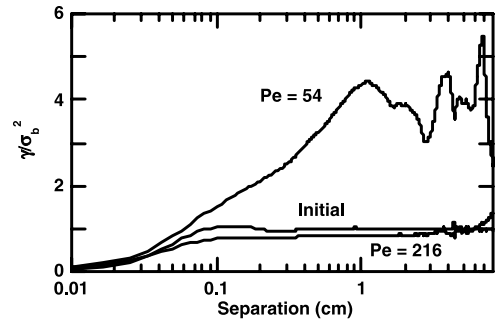

Figure 4. Semivariance normalized by the initial value of σ_b of the fracture aperture field before dissolution (Initial) and after $\langle b \rangle$ had increased to 0.26 mm.

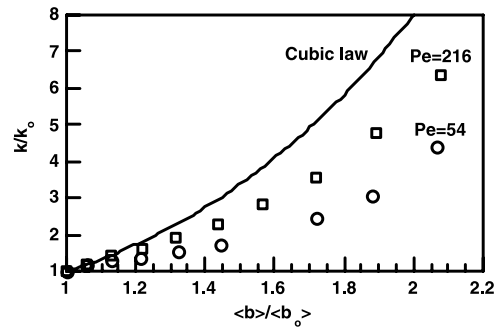

Figure 5. Relative increase in permeability (k/k_o) estimated from simulating flow through the fracture using the Reynolds equation.

median aperture. Otherwise, the distribution is similar to the original aperture distribution. The Pe_o = 216 experiment caused the entire distribution to shift towards larger apertures, but the largest apertures are ~0.3 mm smaller than those in the Pe_o = 54 experiment. Semivariograms (calculated perpendicular to the flow direction) plotted in Figure 4 provide a measure of the change in spatial structure of the aperture fields. For the Pe_o = 54 experiment, the semivariogram is similar to the initial aperture field for separations up to about the correlation length of the initial aperture field

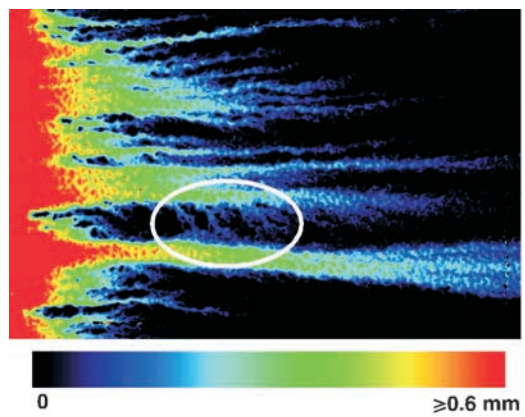

Figure 6. Aperture growth for the Pe_o = 54 experiment when $\langle b \rangle$ = 0.29 mm. The circled region shows the formation of secondary dissolution channels connecting the primary dissolution channel and its neighbor.

(0.8 mm), demonstrating that the small-scale spatial variability of the aperture field was relatively unchanged by dissolution. However, at separations greater than ~0.1 cm, the semivariogram reflects the large-scale, periodic dissolution channels. For the Pe_o = 216 experiment, the semivariogram is a scaled-down version of the semivariogram of the original aperture field, demonstrating that, at the higher flow rate, increased dissolution at small aperture locations caused a decrease in aperture variability at all scales. Thus, the increase in σ_b resulted solely from the fracture-scale trend in the flow direction.

[12] The dissimilar dissolution patterns observed in the two experiments resulted in different rates of permeability increase. We quantify k using Darcy's law

$$Q = -kA(\nabla P)/\mu, \tag{3}$$

where ∇P is the fracture-scale pressure gradient, Q is the flow rate, A is the cross-sectional area of the fracture, and μ is the dynamic viscosity of the fluid. Because the elevation differences between the inflow and outflow reservoirs during the two experiments were fairly small (O(1 cm)), and the inflow/outflow plumbing was long relative to the fracture, we were unable to quantify the pressure gradient in the fracture as precisely as required to evaluate k from (3). Instead, we simulated flow through the measured fracture aperture fields using the Reynolds equation, a two-dimensional approximation to the three-dimensional Stokes equations for flow through a variable aperture fracture (see *Nicholl et al.* [1999] for details). Though detailed measurements of fracture permeability in a similar fracture demonstrated that the Reynolds equation overestimated permeability by about 30% [*Nicholl et al.*, 1999] it provides reasonable estimates of changes in k relative to the initial permeability, k_o. We contrast estimates of k/k_o with those obtained for the cubic law, which assumes that the fracture can be represented as a pair of parallel plates with separation $\langle b \rangle$, resulting in $Q \propto \langle b \rangle^3$ (Figure 5). At $\langle b \rangle / \langle b_o \rangle$ = 2.1 (termination of Pe = 216 experiment), the cubic law predicts a 900% increase in k/k_o, whereas the Pe_o = 216 and 54 experiments exhibited a 670% and 440% increase in k/k_o, respectively. These results demonstrate that for transport-limited dissolution, Pe strongly influences the characteristics of dissolution patterns, which can lead to dramatic differences in fracture permeability.

[13] We continued the Pe_o = 54 experiment until $\langle b \rangle$ = 0.290 mm. As expected, significant growth during the later part of the experiment occurred along the primary dissolution channel (Figure 6). This was in part due to the increased local permeability along this channel. Additionally, it was enhanced by the formation of secondary dissolution channels extending from the neighboring channel towards the primary channel (circled region in Figure 6). These secondary channels served to redirect reactive fluid from the neighboring channel towards the primary channel, effectively enhancing the growth of the primary channel at the cost of its neighbor. The secondary channels form due to a shift in pressure gradients along the primary channel that occurs as the primary channel connects to the outflow end of the fracture. The resulting change in local pressure gradients causes increased flow between the neighboring channel and the primary channel. To our knowledge, the formation of these secondary dissolution channels has not been previously observed experimentally. However, it supports computational results that demonstrate that, at larger scales, such mechanisms can lead to complex branching of dissolution channels significantly influencing growth patterns [*Cheung and Rajaram*, 2002].

4. Concluding Remarks

[14] Experiments in transparent analog fractures have demonstrated that varying Pe_o alone can have a significant influence on the dissolution-induced evolution of aperture variability. At Pe_o = 54, the growth of large-scale dissolution channels dominated the changes in the aperture field, whereas at Pe_o = 216, dissolution occurred more uniformly across the aperture field resulting in reduced short-wavelength aperture variability and a 52% greater increase in permeability. The influence of Pe_o on the spatial structure of dissolution-induced aperture growth clearly plays an important role in the evolution of fracture permeability. Combining systematic experimentation with the development of robust computational models promises further insights into how the underlying mechanisms interact to control dissolution over a broader range of parameters (Pe, Da, and initial aperture variability) and scales.

[15] **Acknowledgments.** We thank Will Peplinski and Dave Ruddle for their assistance with the experiments and Terry Land for providing the KDP samples. Constructive comments from Tim Callahan and an anonymous reviewer greatly improved the manuscript. This work was performed under the auspices of the U. S. Department of Energy by the University of California, Lawrence Livermore National Laboratory under Contract No. W-7405-Eng-48 and Sandia National Laboratory under contract DE-AC04-94AL85000 with funding from the DOE Office of Basic Energy Sciences.

References

Bekri, S., J.-F. Thovert, and P. M. Adler, Dissolution and deposition in fractures, *Engineering Geology*, *48*, 283–308, 1997.

Cheung, W., and H. Rajaram, Dissolution finger growth in variable aperture fractures: Role of the tip-region flow field, *Geophys. Res. Lett.*, *29*(22), 10.1029/2002GL015196, 2002.

Detwiler, R. L., S. E. Pringle, and R. J. Glass, Measurement of fracture aperture fields using transmitted light: An evaluation of measurement errors and their influence on simulations of flow and transport through a single fracture, *Water Resour. Res.*, *35*, 2605–2617, 1999.

Dijk, P. E., B. Berkowitz, and Y. Yechieli, Measurement and analysis of dissolution patterns in rock fractures, *Water Resour. Res.*, *38*(2), 10.1029/2001WR000246, 2002.

Durham, W. B., W. L. Bourcier, and E. A. Burton, Direct observation of reactive flow in a single fracture, *Water Resour. Res.*, *37*(1), 1–12, 2001.

Hanna, R. B., and H. Rajaram, Influence of aperture variability on dissolutional growth of fissures in karst formations, *Water Resour. Res.*, *34*(11), 2843–2853, 1998.

Mullin, J. W., and A. Amatavivadhana, Growth kinetics of ammonium- and potassium-dihydrogen phosphate crystals, *J. Appl. Chem.*, *17*, 151–156, 1967.

Nicholl, M. J., H. Rajaram, R. J. Glass, and R. L. Detwiler, Saturated flow in a single fracture: Evaluation of the Reynolds equation in measured aperture fields, *Water Resour. Res.*, *35*, 3361–3373, 1999.

Stockman, H. W., A lattice gas study of retardation and dispersion in fractures: Assessment of errors from desorption kinetics and buoyancy, *Water Resour. Res.*, *33*(8), 1823–1831, 1997.

Verberg, R., and A. J. C. Ladd, Simulation of chemical erosion in rough fractures, *Phys. Rev. E*, *65*(056311), 1–6, 2002.

R. L. Detwiler and W. L. Bourcier, Lawrence Livermore National Laboratory, PO Box 808, Livermore, CA 94551, USA. (detwiler1@llnl.gov; bourcier1@llnl.gov)

R. J. Glass, Sandia National Laboratories, PO Box 5800, Albuquerque, NM 87185-0735, USA. (rjglass@sandia.gov.)